



**AALBORG UNIVERSITY**  
DENMARK

**Aalborg Universitet**

## **Papers**

*Volume 6: 2001-2003*

Thoft-Christensen, Palle

*Publication date:*  
2007

*Document Version*  
Publisher's PDF, also known as Version of record

[Link to publication from Aalborg University](#)

*Citation for published version (APA):*  
Thoft-Christensen, P. (2007). *Papers: Volume 6: 2001-2003*. Department of Civil Engineering, Aalborg University.

### **General rights**

Copyright and moral rights for the publications made accessible in the public portal are retained by the authors and/or other copyright owners and it is a condition of accessing publications that users recognise and abide by the legal requirements associated with these rights.

- Users may download and print one copy of any publication from the public portal for the purpose of private study or research.
- You may not further distribute the material or use it for any profit-making activity or commercial gain
- You may freely distribute the URL identifying the publication in the public portal -

### **Take down policy**

If you believe that this document breaches copyright please contact us at [vbn@aub.aau.dk](mailto:vbn@aub.aau.dk) providing details, and we will remove access to the work immediately and investigate your claim.

## CHAPTER 121

### FEM MODELLING OF THE EVOLUTION OF CORROSION CRACKS IN REINFORCED CONCRETE STRUCTURES<sup>1</sup>

P. Thoft-Christensen

Aalborg University, Aalborg, Denmark

#### ABSTRACT

Corrosion cracks are caused by the increased volume of corrosion products during the corrosion of the reinforcement. After corrosion initiation the rust products from the corroded reinforcement will initially fill the porous zone near the reinforcement and then result in an expansion of the concrete near the reinforcement. Tensile stresses are then initiated in the concrete. With increasing corrosion, the tensile stresses will at a certain time reach a critical value and cracks will be developed. The increase of the crack width after formation of the initial crack is the subject of this paper. New results based on a Finite Element Analysis (FEM) are presented.

#### 1. INTRODUCTION

Only chloride induced corrosion of the reinforcement is considered. If the rate of chloride penetration into concrete is modelled by Fick's law of diffusion, then it can be shown that the time  $T_{corr}$  to initiation of reinforcement corrosion is

$$T_{corr} = \frac{d^2}{4D} \left( \operatorname{erf}^{-1} \left( \frac{C_{cr} - C_0}{C_i - C_0} \right) \right)^2 \quad (1)$$

where  $d$  is the concrete cover,  $D$  is the diffusion coefficient,  $C_{cr}$  is the critical chloride concentration at the site of the reinforcement,  $C_0$  is the equilibrium chloride concentration on the concrete surface,  $C_i$  is the initial chloride concentration in the concrete,  $\operatorname{erf}$  is the error function. All the parameters mentioned above are modelled by

<sup>1</sup> Proceedings IFIP TC7.5 Conference on "Reliability and Optimization of Structural Systems", Banff, Alberta, Canada, November 2-3, 2003, pp. 221-228.

stochastic variables or stochastic processes; see Thoft-Christensen [1].

With increasing corrosion the tensile stresses will reach a critical value and cracks will be developed. During this process the volume of the corrosion products at initial cracking of the concrete  $W_{crit}$  will occupy three volumes, namely the porous zone  $W_{porous}$ , the expansion of the concrete due to rust pressure  $W_{expan}$ , and the space of the corroded steel  $W_{steel}$ . With this modelling and some minor simplifications it can then be shown that the time from corrosion imitation to crack initiation is; see Liu & Weyers [2]

$$\Delta t_{crack} = \frac{1}{2 \times 0.383 \times 10^{-3} D_{bar} i_{corr}} \left( \frac{\rho_{steel}}{\rho_{steel} - 0.57 \rho_{rust}} (W_{porous} + W_{expan}) \right)^2 \quad (2)$$

where  $D_{bar}$  is the diameter of the reinforcement bar,  $i_{corr}$  is the annual mean corrosion rate,  $\rho_{steel}$  is the density of the steel, and  $\rho_{rust}$  is the density of the rust products. In the derivation of (2) it is assumed that the diameter  $D_{bar}(t)$  of the reinforcement bar at the time  $t$  is modelled by

$$D_{bar}(t) = D_{bar}(T_{corr}) - c_{corr} i_{corr} (t - T_{corr}) \quad (3)$$

where  $c_{corr}$  is a corrosion coefficient.

## 2. SERVICE-LIFE DEFINITIONS

Several different service-life definitions have been proposed in the literature. Four types of definition are:

- (i) Corrosion initiation based definitions
- (ii) Corrosion crack initiation based definitions
- (iii) Corrosion crack width based definitions
- (iv) Spalling based definitions.

All four definitions are illustrated on figure 1 where a deterioration profile and a crack profile are sketched.

Definition (i) is based on an estimation of the corrosion initiation time  $T_{corr}$  and may be written

$$T_{service}^1 = T_{corr} \quad (4)$$

Definition (ii) is based on an estimation of the corrosion crack initiation time  $T_{crack}$  and may be written

$$T_{service}^2 = T_{crack} = T_{corr} + \Delta T_{crack} \quad (5)$$

where  $\Delta T_{crack}$  is the time from corrosion initiation to formation of the first corrosion crack.

Definition (iii) is based on an estimation of the time to formation of a certain corrosion crack width  $T_{crack\ width}$  and may be written

$$T_{service}^3 = T_{crack\ width} = T_{corr} + \Delta T_{crack} + \Delta T_{crack\ width} \quad (6)$$

where  $\Delta T_{crack\ width}$  is the time from corrosion crack initiation to formation of a given critical corrosion crack width.

Definition (iiii) is based on an estimation of the time to first spalling  $T_{spalling}$  and may be written

$$T_{service}^4 = T_{spalling} = T_{corr} + \Delta T_{crack} + \Delta T_{spalling} \quad (7)$$

where  $\Delta T_{spalling}$  is the time from corrosion crack initiation to first spalling.

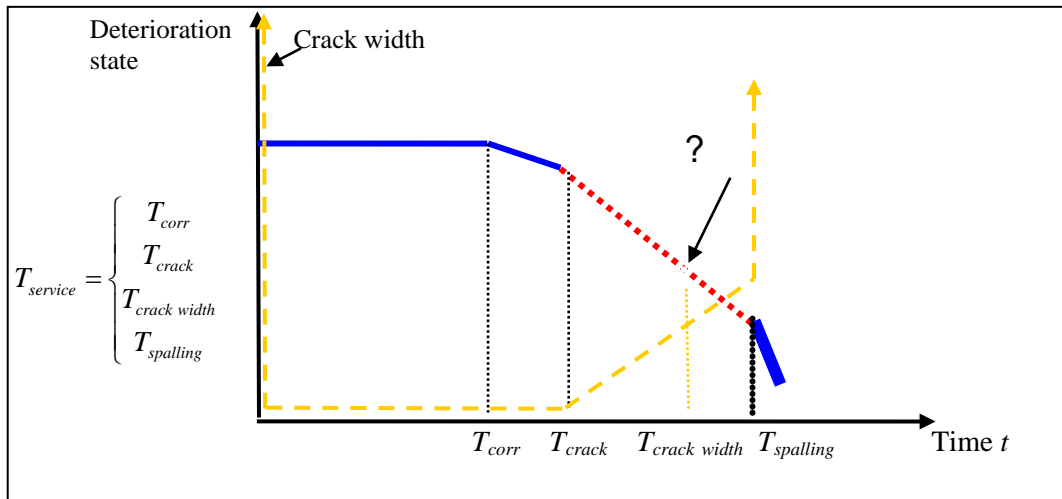


Figure 1. Service-life definitions. “?” indicates the area of major interest in this paper.

### 3. CORROSION CRACK EVOLUTION

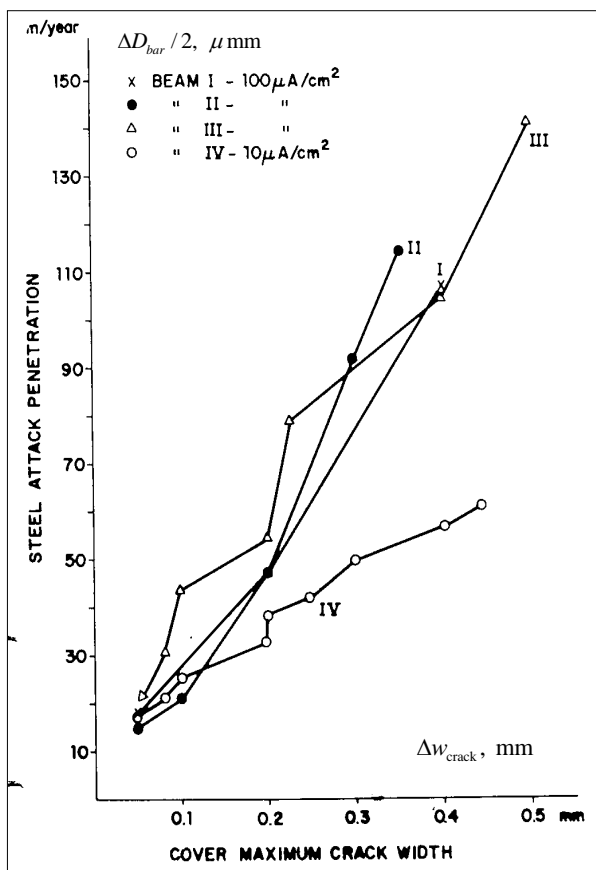


Figure 2. Loss in rebar diameter  $\Delta D_{bar}$  versus the crack width  $\Delta w_{crack}$ . Andrade et al. [3].

After formation of the initial crack the rebar cross-section is further reduced due to the continued corrosion, and the crack width  $w_{crack}$  is increased. Several researchers have investigated the evolution of corrosion cracks in reinforced concrete beams experimentally. In most experiments, see e.g. Andrade et al. [3], the function between the reduction of the rebar diameter  $\Delta D_{bar}$  and the increase of crack width  $\Delta w_{crack}$  measured at the surface of the concrete specimen can be approximated by a linear function.

$$\Delta w_{crack} = \gamma \Delta D_{bar} \quad (8)$$

where  $\gamma$  is the crack width coefficient.

Andrade et al. [3] have investigated experimentally the evolution of corrosion cracks in reinforced concrete beams. In the paper four simple test specimens have been investigated. In all four experiments the function between the reduction of the rebar diameter and the maximum crack width measured in the surface of the concrete specimen can be approximated by a linear function, see figure 2. The crack width coefficient  $\gamma$  depends on the cross-sectional data and is of the order 1.5 to 5.

#### 4. FEM ESTIMATION OF THE CRACK WIDTH COEFFICIENT $\gamma$

##### 4.1 The FEM estimation in reference [4]

For illustration purposes the coefficient  $\gamma$  in equation (4) was estimated using FEM analysis by Thoft-Christensen [4] using FEMLAB/MATLAB. A rectangular beam cross-section with only one reinforcement bar was considered, see figure 2. The diameter of the hole around the rebar at the time of crack initiation is  $D_{hole} = 20$  mm and that the cover is  $c = 10$  mm. The initial crack width is 0.01 mm.

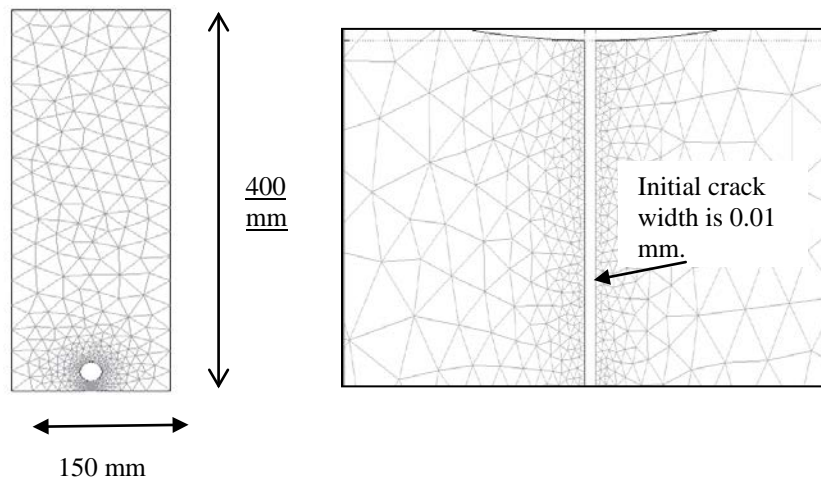


Figure 3. FEM net. The total net to the left and the local net near the crack to the right.

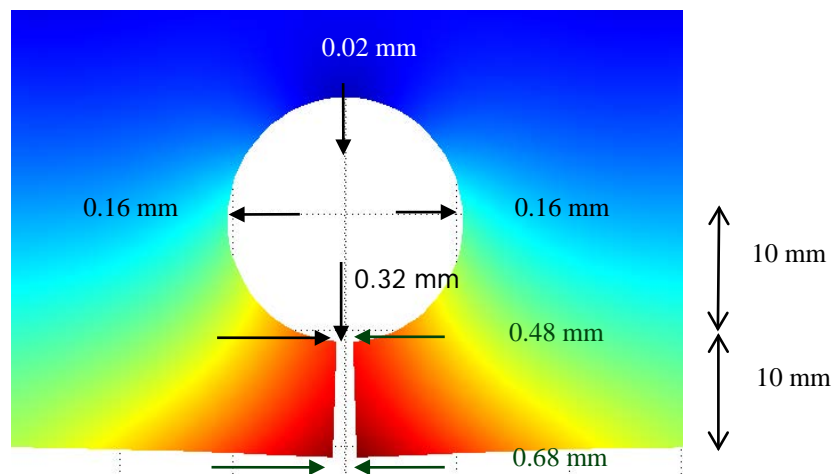


Figure 4. Displacements at four points of the circular hole and at the ends of the crack. Magnification factor is 3.

In the FEM modelling the rectangular cross-section is assumed to have a hole at

the location of the reinforcement and a crack (0.01 mm) from the hole to the boundary. The number of constant strain elements is 5580 and there are 3066 nodes. The material is assumed to be linear elastic with the elasticity module  $E = 25 \times 10^9$  Pa and the pressure from the increasing corrosion products is modelled as a uniform loading (pressure)  $p = 1 \times 10^8$  N/m at the boundary of the hole. The result of the analysis is shown in figure 3. The increase in the crack width in the considered time interval  $\Delta t$  is  $\Delta w_{crack} = 0.67$  mm and the average increase in the hole diameter is  $\Delta D_{hole} = 0.31$  mm.

The produced volume (area) of the corrosion products  $W_{rust}$  is related to the corroded steel volume (area)  $W_{steel}$  by  $W_{rust} = \alpha W_{steel}$ , where  $\alpha = \rho_{rust} / \rho_{steel}$  (the relation between the densities of the rust product and the steel) depends on the type of corrosion products. Typical values are 2 - 4. Therefore,

$$\begin{aligned} (\alpha - 1)\pi\Delta D &= \pi\Delta D_{hole} + \varepsilon \Rightarrow (\alpha - 1)\pi\gamma^{-1}\Delta w = \pi\eta^{-1}\Delta w + \varepsilon \\ \text{so } \gamma &< (\alpha - 1)\eta \\ \text{and } \gamma &\approx (\alpha - 1)\eta \text{ for small } \varepsilon \end{aligned} \quad (9)$$

where  $\varepsilon$  is the amount of rust in the increased crack.

For the example shown in figure 3 one gets

$$\begin{aligned} 0.67 &= \eta \times 0.31 \Rightarrow \eta = 2.2 \\ \gamma < (\alpha - 1) \times 2.2 &= \begin{cases} 1.1 \times 2.2 = 2.4 \text{ for black rust } \text{Fe}_3\text{O}_4 \\ 3.1 \times 2.2 = 6.8 \text{ for brown rust } \text{Fe}(\text{OH})_3 \end{cases} \end{aligned} \quad (10)$$

These  $\gamma$ -values are of the same magnitude as the experimental values presented in section 2.

#### 4.2 Rectangular beam with one symmetrical rebar

In this section the results of FEM analysis of the cross-section illustrated in figure 5 are presented with 10 different combinations of the cover  $c$  and the diameter  $D$  of the hole.

The 10 designs A-J are defined and the displacements of the points 1-7 for each design are shown in table 1. The estimates of the coefficients  $\eta$  and  $\gamma$  are shown in table 2.

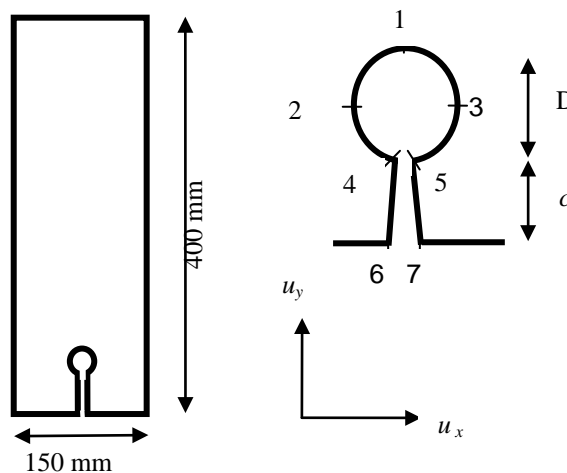


Figure 5. Cross-section geometry and numbering of points where displacements are estimated.

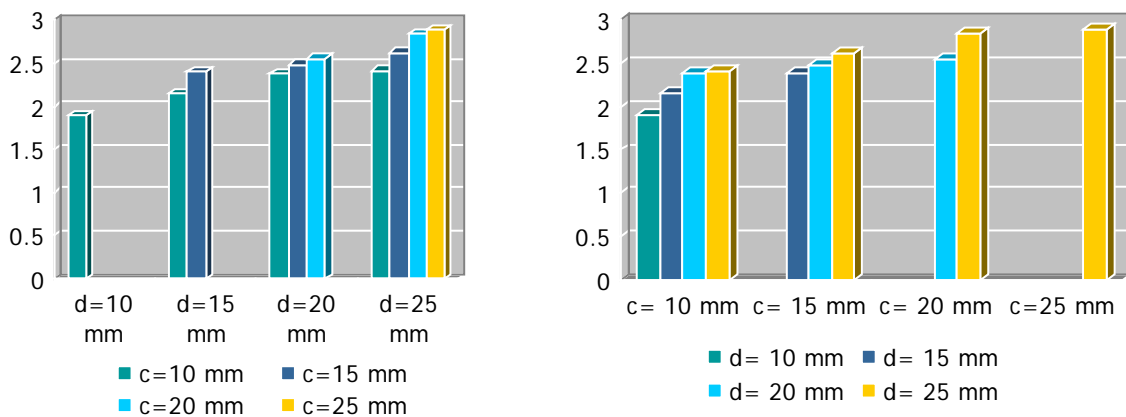
Design	D	c	1		2 and 3		4 and 5		6 and 7	
			$u_x$	$u_y$	$u_x$	$u_y$	$u_x$	$u_y$	$u_x$	$u_y$
<b>A</b>	10	10	0	0.00	-0.06	-0.40	-0.07	-0.10	-0.10	-0.09
<b>B</b>	15	10	0	-0.01	-0.11	-0.70	-0.14	-0.19	-0.20	-0.18
<b>C</b>	20	10	0	-0.03	-0.16	-0.11	-0.23	-0.32	-0.34	-0.31
<b>D</b>	25	10	0	-0.04	-0.24	-0.15	-0.35	-0.50	-0.52	-0.49
<b>E</b>	15	15	0	-0.01	-0.10	-0.06	-0.13	-0.16	-0.19	-0.14
<b>F</b>	20	15	0	-0.24	-0.16	-0.10	-0.22	-0.26	-0.32	-0.24
<b>G</b>	25	15	0	-0.04	-0.22	-0.15	-0.32	-0.41	-0.48	-0.40
<b>H</b>	20	20	0	-0.02	-0.17	-0.10	-0.22	-0.24	-0.33	-0.22
<b>I</b>	25	20	0	-0.04	-0.24	-0.15	-0.34	-0.37	-0.52	-0.35
<b>J</b>	25	25	0	-0.04	-0.25	-0.15	-0.34	-0.35	-0.53	-0.33

Table 1. Estimated displacement of points 1-7 in designs A-J.

	A	B	C	D	E	F	G	H	I	J
$\eta$	1.73	1.95	2.16	2.19	2.18	2.25	2.38	2.32	2.58	2.63
$\gamma_{black}$	1.90	2.15	2.38	2.41	2.40	2.48	2.62	2.55	2.84	2.89

Table 2. Estimated values for  $\eta$  and  $\gamma$  in the case of black rust.

In figure 5 is to the left shown values of  $\gamma$  (black rust) for fixed diameter  $d$  as a function of the cover  $c$ .  $\gamma$  increases with the cover  $c$ . To the right is shown values of  $\gamma$  (black rust) for fixed cover  $c$  as a function of the diameter  $d$ .  $\gamma$  increases with the diameter  $d$ .

Figure 6.  $\gamma$  for black rust.

## 5. SPALLING

In this section it is shown on the basis of a number of examples how FEM analysis may help in estimating how and where new corrosion cracks are established with continuing corrosion after the initial (first) crack is formed.

In Figure 7 a beam with a single non-symmetrical rebar and an initial crack from the rebar to the lower side of the beam is considered. The FEM method is used similarly to the examples shown earlier. The maximum tensile stress at the boundary of the hole occur in the NE direction indicating that the next crack may occur in that direction. In figure 8 the same beam is shown, but now with two symmetrical rebars. New corrosion

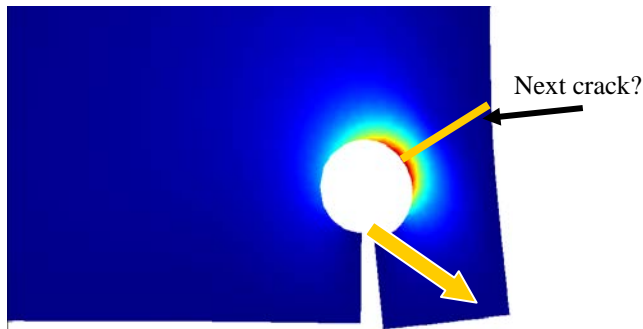


Figure 7. Beam with non-symmetrical rebar.

cracks seem to occur in the same direction as shown in figure 7 resulting in spalling at the two corners, see the picture in the middle where the first principal stresses are shown. The picture to the right shows the stresses in the  $y$ -direction (vertical direction). They seem to show that the next spalling will be a vertical displacement of the middle section.

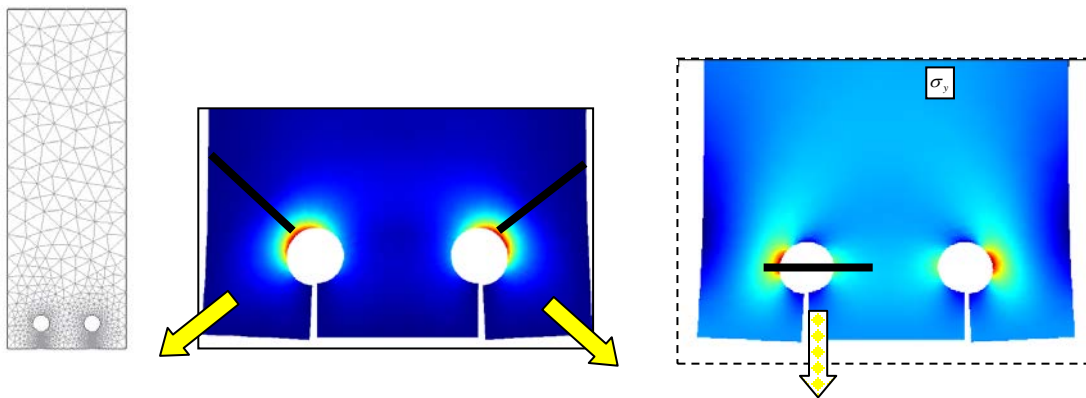


Figure 8. Beam with two symmetrical rebars.

In figure 9 is shown a similar case is shown, but now with three rebars. Again, the analysis seems to indicate that the spalling will first occur at the two corners and then at the two middle sections.

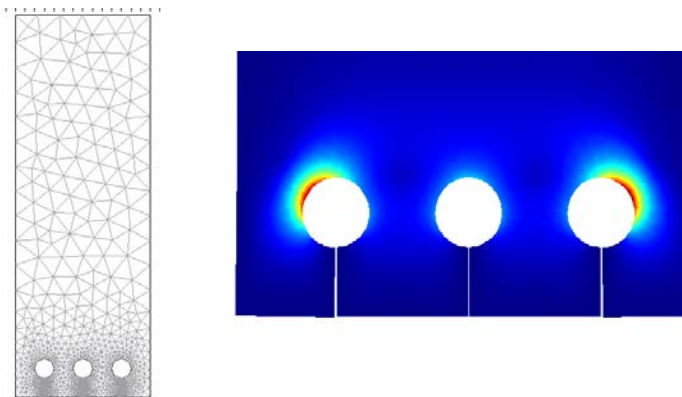


Figure 9. Beam with three symmetrical rebars.

In the last example a reinforced concrete bridge deck with six rebars is considered, see figure 9. The analysis seems to indicate again that the spalling will first occur at the two corners and then at the five middle sections.



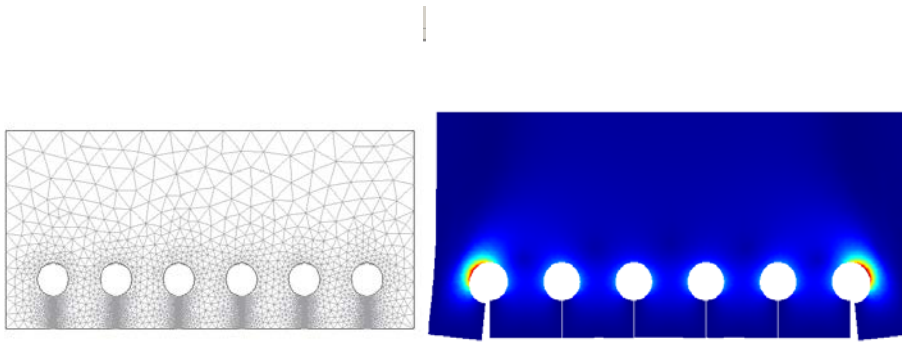


Figure 10. Reinforced concrete bridge deck with six rebars.

## 6. CONCLUSIONS

Modelling of corrosion crack initiation and corrosion crack evolution is presented with special emphasis on modelling of the crack evolution. Experiments and FEM analysis seem to show that the function between the reduction of the rebar diameter  $\Delta D_{bar}$  and the corresponding increase in crack width  $\Delta w_{crack}$  in a given time interval  $\Delta t$  measured on the surface of the concrete specimen can be approximated by a linear function, and it is demonstrated how the crack width coefficient  $\gamma$  can be estimated using FEM analysis.

## 7. ACKNOWLEDGEMENT.

The author is grateful to Professor Staffan Svensson, Aalborg University for assistance with the FEM analyses.

## 8. REFERENCES

- [1] Thoft-Christensen, P. (2001). What Happens with Reinforced Concrete Structures when the Reinforcement Corrodes? Keynote Speech at the 2<sup>nd</sup> International Workshop on “Life-Cycle Cost Analysis and Design of Civil Infrastructure Systems”, Ube, Yamaguchi, Japan, September 27-29, 2001. Proceedings: Maintaining the Safety of Deteriorating Civil Infrastructures, pp. 293-304.
- [2] Liu, Y. & R.E. Weyers (1998). Modelling of the Time to Corrosion Cracking in Chloride Contaminated Reinforced Concrete Structures. ACI Materials Journal, Vol. 95, pp. 675-681.
- [3] Andrade C., Alonso, C. & Molina, F.J. (1993). Cover Cracking as a Function of Bar Corrosion: Part 1-Experimental Test. Materials and Structures, Vol. 26, pp. 453-464, 1993.
- [4] Thoft-Christensen, P. (2003). Modelling Corrosion Cracks. IFIP TC7 Conference on “System Modeling and Optimization”, Sophia Antipolis, France, July 21-25, 2003.